Mathematics Research Reports

Boris Hasselblatt, Curtis Heberle

Hyperbolicity from contact surgery

Volume 4 (2023), p. 1-10.

https://doi.org/10.5802/mrr.14

Mathematics Research Reports *is member of the*
Centre Mersenne for Open Scientific Publishing
www.centre-mersenne.org
e-ISSN: 2772-9559

Mathematics **R**esearch **R**eports
Volume 4 (2023), 1–10

Hyperbolicity from contact surgery

Boris Hasselblatt & Curtis Heberle

(Recommended by Svetlana Katok)

Abstract. A Dehn surgery on the *periodic* fiber flow of the unit tangent bundle of a surface produces a uniformly *hyperbolic* Cantor set for the resulting contact flow.

1. Introduction

This note augments recent progress at the intersection of dynamical systems and contact geometry centered on a Dehn surgery construction adapted to Reeb flows ("contact flows" to dynamicists) [7]. This surgery is known to contact-symplectic topologists as a Weinstein surgery, and its introduction in [6] makes it easier to study dynamical properties (as opposed to, for instance, topological properties). We explicitly establish here that when performed on a trivial flow, this surgery can produce hyperbolicity: the flow being surgered is the (strictly periodic) fiber flow on the unit tangent bundle of a surface, and hyperbolicity ensues when the surgery is performed along a sufficiently nontrivial annulus. It is explicitly manifested as a Smale horseshoe. This complements the recent discovery that nondegenerate Reeb flows on closed irreducible oriented 3-manifolds other than graph manifolds have positive topological entropy [2].

From the perspective of a dynamicist or topologist the creation of dynamical or topological complexity through surgery is not new. The suspension construction (or mapping torus) can be viewed as starting from the obvious S^1-action on $M \times S^1$ and performing surgery along $M \times \{0\}$ with a dynamically complex identification map on M, such as $M = \mathbb{T}^2$, $f = \left(\begin{smallmatrix} 2 & 1 \\ 1 & 1 \end{smallmatrix}\right)$. In this case, the complexity of the resulting $\mathbb{R}$-action matches that of f. Topologists are interested in this construction as a source of new manifolds, while dynamicists see it as a source of examples of flows—whose dynamics is a close counterpart to the discrete-time dynamics of the underlying map. The introduction of the dynamical contact surgery in [6] was motivated by the exotic flows it produces when applied to a (hyperbolic) geodesic flow. Later, [7] showed how it can produce (possibly slightly) larger complexity on an exponential scale. The present application produces the same manifolds, but creates hyperbolicity, hence exponential orbit complexity, from an S^1-action, the most trivial of flows.

The present construction differs from previous ones in several ways. Unlike the suspension construction, this surgery is performed on a contact flow (that is, the Reeb flow of a contact form), the fiber flow on the unit tangent bundle of a surface and produces a new contact flow. Contact flows are the canonical opposite of suspension flows. On the other hand, the resulting complexity far exceeds both that of the identification map on the surgery annulus and that of the original flow. A like surgery on the fiber flow was undertaken in [7] on an annulus in the unit tangent bundle of a surface that projects injectively under the footpoint projection to the surface (to a neighborhood of a simple

Received August 11, 2022; revised January 22, 2023.
2020 *Mathematics Subject Classification.* 37D20, 57N10.
Keywords. Hyperbolic flow, 3-manifold, contact flow, surgery.

closed geodesic). In that context, the resulting flow has the same complexity as the identification map, which is larger than that of the fiber flow on which the surgery is being performed; it has quadratic orbit growth.

Here, we instead consider an annulus that projects to a neighborhood of a *self-intersecting* geodesic, and the resulting overlap produces hyperbolicity. The mechanism is that of linked twist maps [1, 3, 4, 8–15] to which an introduction is given in [12, Section 1.2.2] and in [14]. We note that the insights about linked twist maps that are salient for this and likely future work are some 40 years old [1, 3, 4, 10, 15], and that the self-linked twists involved here are counter-oriented, which is the less straightforward of the two possibilities, as intimated by Remark 1 on page 9.

Main Theorem. *Consider the (periodic) fiber flow of the unit tangent bundle of a negatively curved surface and an annulus defined by a nonsimple closed geodesic. A Dehn–Foulon–Hasselblatt–Vaugon–Weinstein surgery [7] of this flow along this annulus gives a contact flow which exhibits a Smale horseshoe for* $(1,k)$*-Dehn twisting ("*k*-twist" for short) with* $k \geq 3$*. This implies exponential orbit growth and positive topological entropy.*

This appears to be a new way of constructing flows with a hyperbolic set, particularly among Reeb flows, and this theorem was announced in [7]. Here, we focus on the geometric and dynamical features of the surgery rather than the contact structure, since that is done carefully in [7]. Establishing the dynamical complexity, that is, the presence of a horseshoe, does not need to make any reference to this nature of the fiber flow. Nor does it require describing the flow with great precision. Indeed, horseshoes are robust under C^1-perturbation.

The flows we construct are periodic on a large set, namely on the union of those fibers which do not meet the surgery annulus. Consequently, the resulting flow is not hyperbolic in the usual sense [5]—the chain recurrent set includes this large periodic piece and is hence not hyperbolic. For the same reason the Liouville volume is (invariant but) not ergodic, nor hyperbolic. It is a separate project to show that the (Liouville) volume restricted to the orbit-saturation of the surgery annulus is hyperbolic and ergodic (indeed, Bernoulli, along the lines of [1, 4, 15], but adapted to the inconvenient counter-orientation of the linked twist maps as in [10]). This is not that project.

We produce a horseshoe, analogously to [3], as follows. Section 2 describes the surgery construction, with a little more background on the ambient contact structures than needed for the proof of the theorem (because the contact nature of the surgery was already established in [7]). Section 3 produces the horseshoe engendered by the surgery, specifically a rectangle in the surgery section which is mapped across itself in at least two strips by the return map to the section. To establish hyperbolicity of the compact isolated set defined by this, Section 4 describes how the return map is akin to classical linked twist maps, albeit counter-oriented rather than co-oriented. Finally, Section 5 then produces the invariant (and automatically expanding) cone family, which gives hyperbolicity by the Alexeev cone criterion [5]. At the end we return to a discussion of the context and of possible further work.

2. Description of the surgery

We build on [7, Section 8], which describes a surgery construction adapted to Reeb flows ("contact flows" for dynamicists). This construction was originally conceived as a source of uniformly hyperbolic Reeb flows constructed from the (hyperbolic) geodesic flow. Here we apply it to the (periodic!) fiber (or vertical) flow in a unit tangent bundle $M = S\Sigma$ of a surface Σ of negative and (for convenience of exposition) constant curvature equipped with its natural contact structures.

Although this is not essential, we introduce the three Reeb flows that naturally appear on the unit tangent bundle of a surface of constant negative curvature [5, Chapter 2]. This is elementary but not commonly presented. There is a canonical framing consisting of X, the vector field on $S\Sigma$ that generates the geodesic flow, of V, the vertical vector field (pointing in the fiber direction and defined uniquely by a choice of orientation), and of the horizontal vector field $H := [V, X]$. It satisfies the classical *structure equations*

$$[V, X] = H, \quad [H, X] = V, \quad [H, V] = X. \tag{2.1}$$

One can check these by using that in the $\mathrm{PSL}(2,\mathbb{R})$-representation of $S\widetilde{\Sigma}$, these vector fields are given by

$$X \sim \begin{pmatrix} 1/2 & 0 \\ 0 & -1/2 \end{pmatrix}, \quad H \sim \begin{pmatrix} 0 & 1/2 \\ 1/2 & 0 \end{pmatrix}, \quad V \sim \begin{pmatrix} 0 & -1/2 \\ 1/2 & 0 \end{pmatrix}.$$

The structure equations imply that $e^{\pm} := V \pm H$ satisfies $[X, V \pm H] = \mp e^{\pm}$, so if a vector field $f \cdot e^{\pm}$ along an orbit of X is invariant under the geodesic flow, then $0 = [X, fe^{\pm}] = (\dot{f} \mp f)e^{\pm}$, where $\dot{f}$ is the derivative along the orbit. This means that $\dot{f} = \pm f$, so $f(t) = \mathrm{const} \cdot e^{\pm t}$. Thus, the differential of the geodesic flow expands and contracts, respectively, the directions $e^{\pm}$; this is the Anosov property and $E^{\pm}$ is spanned by the vector $e^{\pm} = V \pm H$.

Of course, in the $\mathrm{PSL}(2,\mathbb{R})$-representation of $S\widetilde{\Sigma}$, these three flows are given by

$$\begin{aligned} X &\rightsquigarrow \exp\left(\begin{pmatrix} 1/2 & 0 \\ 0 & -1/2 \end{pmatrix} t\right) = \begin{pmatrix} e^{t/2} & 0 \\ 0 & e^{-t/2} \end{pmatrix}, \\ H &\rightsquigarrow \exp\left(\begin{pmatrix} 0 & 1/2 \\ 1/2 & 0 \end{pmatrix} t\right) = \begin{pmatrix} \cosh t/2 & \sinh t/2 \\ \sinh t/2 & \cosh t/2 \end{pmatrix}, \\ V &\rightsquigarrow \exp\left(\begin{pmatrix} 0 & -1/2 \\ 1/2 & 0 \end{pmatrix} t\right) = \begin{pmatrix} \cos t/2 & -\sin t/2 \\ \sin t/2 & \cos t/2 \end{pmatrix}. \end{aligned}$$

To see in these terms that X is a Reeb field, define a 1-form α_0 by $\alpha_0(X) = 1$ and $\alpha_0(V) = 0 = \alpha_0(H)$. For $Z \in \{V, H\}$ we have

$$\mathrm{d}\alpha_0(X, Z) = \underbrace{\mathscr{L}_X \overbrace{\alpha_0(Z)}^{\equiv 0}}_{=0} - \underbrace{\mathscr{L}_Z \overbrace{\alpha_0(X)}^{\equiv 1}}_{=0} + \underbrace{\alpha_0(\overbrace{[Z, X]}^{\in\{V,H\}})}_{=0} = 0,$$

so $\iota_X \mathrm{d}\alpha_0 \equiv 0$. Additionally $\alpha_0 \wedge \mathrm{d}\alpha_0(X, V, H) = \alpha_0(X)\,\mathrm{d}\alpha_0(V, H) = 1$ because

$$\mathrm{d}\alpha_0(V, H) = \underbrace{\mathscr{L}_V \overbrace{\alpha_0(H)}^{\equiv 0}}_{=0} - \underbrace{\mathscr{L}_H \overbrace{\alpha_0(V)}^{\equiv 0}}_{=0} + \underbrace{\alpha_0(\overbrace{[H, V]}^{=X})}_{=1} = 1.$$

Thus, $\alpha_0 \wedge \mathrm{d}\alpha_0$ is a volume form; in fact, a volume particularly well adapted to this canonical framing, and α_0 is a contact form with $X = R_{\alpha_0}$.

Likewise, one can check that the 1-forms $\beta = -d\alpha_0(H, \cdot)$ and $\gamma = d\alpha_0(V, \cdot)$ defined by $\beta(V) = 1$ and $\beta(X) = 0 = \beta(H)$, and $\gamma(H) = 1$ and $\gamma(X) = 0 = \gamma(V)$ are contact forms with Reeb vector fields $R_\beta = V$ and $R_\gamma = H$. Note that the orientation given by $\beta \wedge d\beta$ is the opposite of the orientation given by $\alpha_0 \wedge \mathrm{d}\alpha_0$; therefore α_0 and β define different contact structures. Dynamically R_{α_0} and R_β are polar opposites: the geodesic flow is hyperbolic and the fiber flow is periodic.

To fix ideas in a convenient way, we suppose that the surface Σ has genus two and constant curvature, and that the closed geodesic $\mathfrak{c}\colon S^1 \to \Sigma$, $s \mapsto \mathfrak{c}(s)$ we use to define the surgery annulus is as shown in Figure 1, with a single self-intersection at right angles. Consider the knot γ obtained by rotating the unit vector field along $\mathfrak{c}$ by the angle $\theta = \pi/2$. This knot is Legendrian since H is tangent to γ. To obtain standard coordinates in a neighborhood of γ we first consider an annulus A in $S\Sigma$ transverse to the fibers with

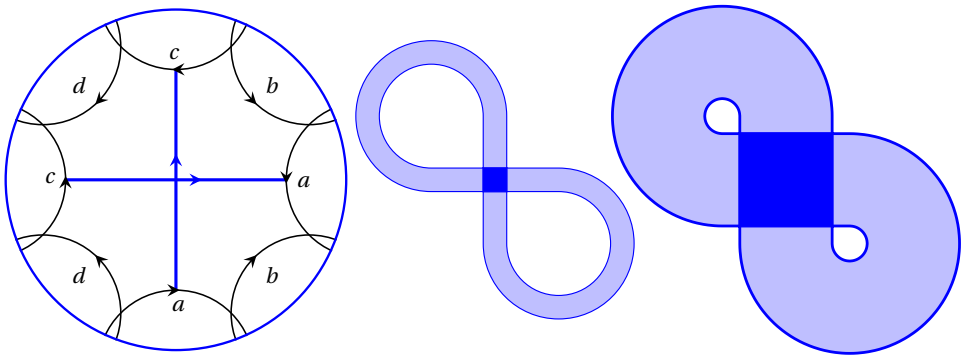

Figure 1. A self-intersecting geodesic and projections of surgery annuli with different widths

coordinates $(s,w)\in S^1\times(-2\epsilon,2\epsilon)$ such that $\beta_{|A}=w\,ds$ and then flow along the Reeb vector field R_β to obtain coordinates $(t,s,w)\in S^1\times A=N$ such that $\beta=dt+w\,ds$.

This is more detail than needed here. It suffices that we have defined a smooth embedding ι of the "abstract" annulus $\mathbb{A}:=\mathbb{R}/\mathbb{Z}\times[0,1]$ into the unit tangent bundle such that the image projects along fibers as shown in Figure 1; under the base-point projection, this corresponds to a tubular neighborhood of $\mathfrak{c}$.

Next, define a twist f on $\mathbb{A}$. For purposes of the present description it can either be linear or smoothly tangent to the identity on the boundary. The twist $\iota\circ f\circ\iota^{-1}$ on $\iota\mathbb{A}$, taken as an identification map, defines the surgery. (In the sequel we will conflate this and f. How to ensure that the surgered flow is a Reeb flow is described carefully in [7].) We denote the surgered manifold by $M_{\iota,f}$. Note that the unit tangent spheres at points outside of the projection to Σ of the annulus are unaffected by the surgery. The embedded annulus $\iota\mathbb{A}$ is a section for the surgered flow, and we will henceforth study the restriction to the orbits that meet this section, and we will do so by studying the return map to this section $\iota\mathbb{A}$.

3. Horseshoe

We begin by locating those points which always return to the overlap region and are hence subject to twists in alternating orientation. We then show that this implies hyperbolicity. Specifically, we here look for a rectangle which is mapped across itself in a manner analogous to the Smale horseshoe in Figure 2.

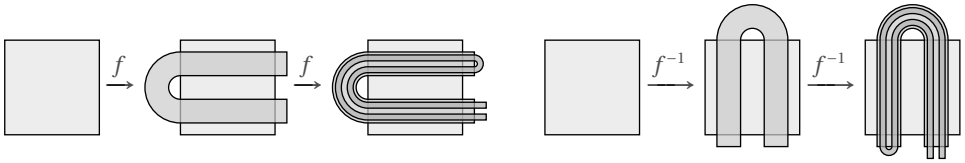

Figure 2. Horseshoe (from [5] with permission)

In doing so, consider Figure 3. It shows a k-twist f with $k=2$ of the embedded annulus.[1] The corners of the "overlap" square are denoted by A,B,C,D; on the top copy of that region, the twist is in the vertical direction. In that copy, denote by γ_1 the curve

[1] $k=2$ reduces clutter but is insufficient; the invariant set $\Lambda:=\bigcap_{i\in\mathbb{Z}}f^i(Q)$ is a hyperbolic fixed point rather than a hyperbolic Cantor set. Figure 4 shows a less trivial situation, but we refer to the notations in Figure 3.

with end-points at D and on the line AB, respectively, such that $f(\gamma_1) \subset CD$, and by γ_2 the curve with end-points at B and on CD, respectively, such that $f(\gamma_2) \subset AB$. Likewise, on the bottom copy, where the twist is in a horizontal direction, let σ_1 be the curve from D to BC such that $f^{-1}(\sigma_1) \subset AD$ and σ_2 the curve from B to AD such that $f^{-1}(\sigma_2) \subset BC$. Let Q denote the quadrilateral in the top layer bounded by the curves γ_1, γ_2, σ_1 and σ_2, and let Q' denote the corresponding quadrilateral in the bottom layer.

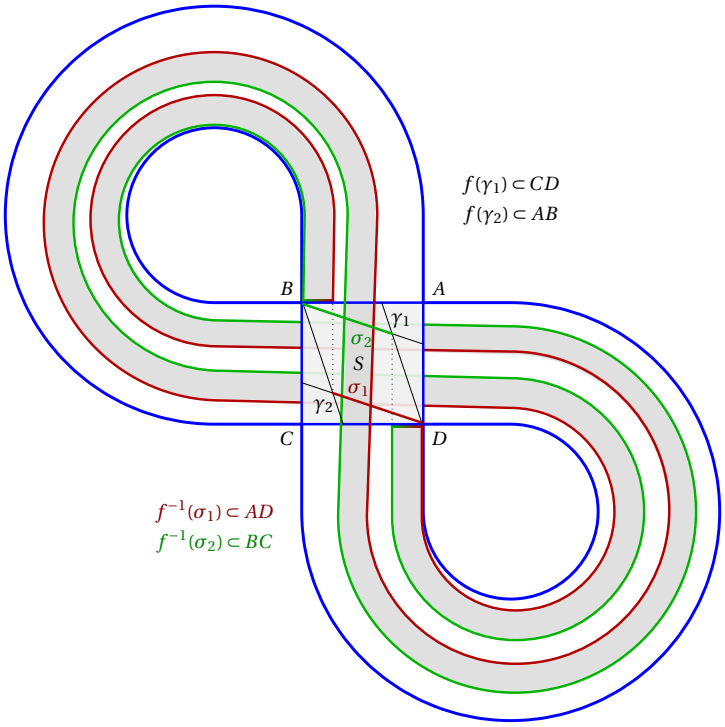

FIGURE 3. Self-linked 2-twist

The strip snaking across the annulus is $f(Q)$ as follows. The sides γ_1 and γ_2 are mapped into CD and AB, respectively, while the sides σ_1 and σ_2 are wrapped around the annulus k times, so $f(Q)$ is a narrow strip beginning on AB and terminating on CD having k intersections with Q' and $k-1$ intersections with Q; in Figure 3, this is the one intersection labeled S. Our interest is in $f(Q) \cap Q$, because its points are subject to a vertical twist followed by a horizontal one after the flow takes Q to Q'.

For $k > 2$ this overlap produces two or more strips of Q mapped across Q as in Figure 2. We will show that the invariant set $\Lambda := \bigcap_{i \in \mathbb{Z}} f^i(Q)$ is hyperbolic.

4. Relationship with linked twist maps

With respect to these pictures, let us assume that ι is "linear" in that it maps the boundary and each line $\{x\} \times [0,1]$ with constant speed, and the image of each of these lines is a line orthogonal to the boundary. Since this assumption is only used on the invariant set from the previous section, it does not preclude smoothness—the surgery can be smoothed in a neighborhood of the annulus boundary which is disjoint from this invariant set.

Again, this annulus is a section for the fiber flow. The surgery uses the twist f (conjugated by ι). This connects fiber segments ending (in the sense of the flow direction) at

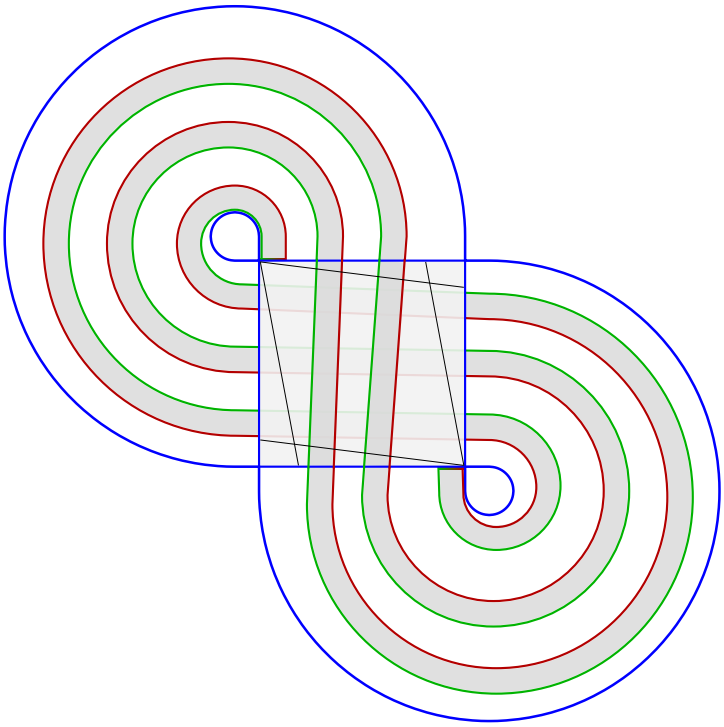

Figure 4. Self-linked 3-twist

a point z in the annulus with segments starting at $f(z)$. The original flow corresponds to $f = \mathrm{Id}$. The return map of the surgered flow to this section then has twist dynamics plus the interaction of transverse twists in the blue "overlap" square. Here is a slightly inaccurate description of the dynamics which shows the close kinship with classical linked twist maps. The subsequent proof of hyperbolicity does not use this description.

Figure 5 shows how the embedded annulus corresponds to two strips in the plane with suitable identifications; these are shown in enclosing squares labeled H and V according to whether the included strip is horizontal or vertical. Let $J = J^{-1}$ denote the piecewise

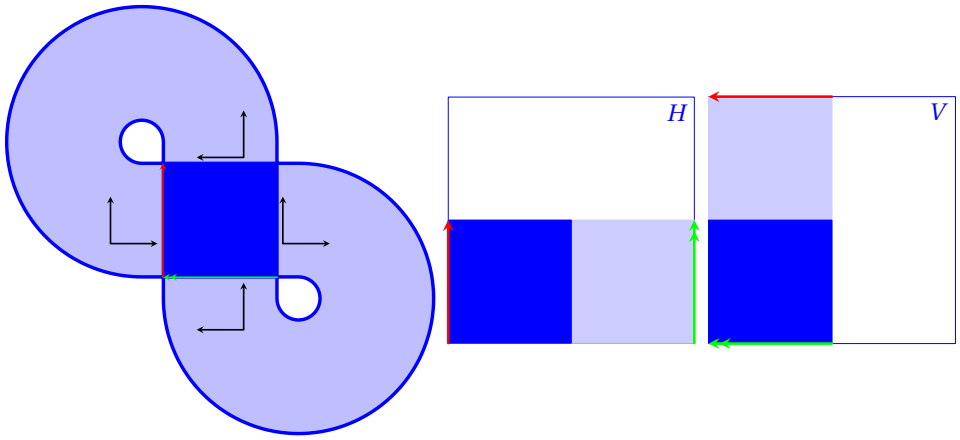

Figure 5. Overlap and identifications of the surgery annulus

isometric involution that interchanges H and V by translations. The strips correspond to $[0,1]\times[0,1/2]$ and $[0,1/2]\times[0,1]$, respectively, in a natural way; say, up to translation, rotation, and scaling. Each is marked with the blue "overlap" square from the projection.

Define $F\colon H\cup V\to H\cup V$ by $J\circ f$ on the union of the strips (as representing the surgery annulus) and J elsewhere. The linked twist map in question is defined by $T:=F\circ F$. This is as smooth as f.

To see that this represents the return map of the flow, consider first a point z in H outside the strip. Then $F(z)=J(z)$, which may lie outside the strip in V, in which case $T(z)=J^2(z)=z$. If $F(z)=J(z)$ lies in the strip in V, then $T(z)=F(J(z))$. Similarly with points in V outside the strip.

If $z\in H$ is in the strip, then $f(z)$ is in one of the strips, so $F(z)$ is in a strip *only* if it lies in either of the "overlap" squares, in which case $T(z)=F(F(z))$ involves four nontrivial maps, including two twists in orthogonal directions; otherwise $T(z)=J(F(z))$. Similarly for $z\in V$ in the strip.

So indeed, the "overlap" square is the locus of composing orthogonal twists. The sole inaccuracy in this description is that the rotation between twist of one kind and the other is not unique but only defined up to a sign (or an angle of π) depending on whether the transition is from top to bottom or vice versa.

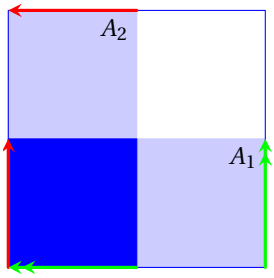

FIGURE 6. Linking of twists

5. Hyperbolicity

For establishing hyperbolicity of the horseshoe, we briefly continue with the preceding description, and place H and V in Figure 5 on top of each other to obtain a representation in the unit square $[0,1]^2$ with the overlap square $[0,1/2]^2$ in the lower left corner as in Figure 6. The twist f which defines the surgery can be defined in terms of an $\mathfrak{f}\colon[0,1/2]\to\mathbb{R}$ such that

- $\mathfrak{f}$ is smooth,
- $\mathfrak{f}(0)=0$,
- $\mathfrak{f}(1/2)\in\mathbb{N}$,
- $\mathfrak{f}'\geq 0$,
- $\exists\,\epsilon>0,\ \Delta>2$ such that $\mathfrak{f}'(x)>\Delta$ when $\epsilon\leq x\leq 1/2-\epsilon$.

In our context, we can take $\Delta=k\geq 3$. Taking as in Figure 6 the two parts of the surgery annulus to be

$$A_1:=\left\{(x,y)\in[0,1]^2\,\middle|\,0\leq y\leq 1/2\right\},\quad A_2:=\left\{(x,y)\in[0,1]^2\,\middle|\,0\leq x\leq 1/2\right\},$$

this produces (area- and orientation-preserving integrable twist) maps by projecting

$$F\colon(x,y)\mapsto\begin{cases}(x+\mathfrak{f}(y),y) & \text{if } y\leq 1/2\\ (x,y) & \text{if } y>1/2.\end{cases},\qquad G\colon(x,y)\mapsto\begin{cases}(x,y-\mathfrak{f}(x)) & \text{if } x\leq 1/2\\ (x,y) & \text{if } x>1/2\end{cases}\tag{5.1}$$

to $[0,1]^2$ according to the identifications in Figure 6. With respect to these choices, the return map is given up to a sign by the linked twist map T defined by the projection of $G\circ F$, and (for small ϵ), the set Λ consists of those (x,y) for which $T^n(x,y)\in[\epsilon,\frac12-\epsilon]^2$ for all $n\in\mathbb{Z}$.

While the preceding is not an exact description of the dynamics, it suffices for establishing hyperbolicity because either way, the differential of the second iterate of the return map is either $DG\circ DF$ or $-DG\circ DF$, depending on the point. An alternative way of seeing this without reference to linked twist maps is by turning attention to the frame field on the annulus, which is illustrated in the left half of Figure 5. Applying the twist F, then changing layers in the overlap region, then applying the complementary twist and changing layers again produces a map whose differential is $DT=\pm JDGJDF$, where J is the rotation by π and the sign depends on the point—and is immaterial for invariance of cones.

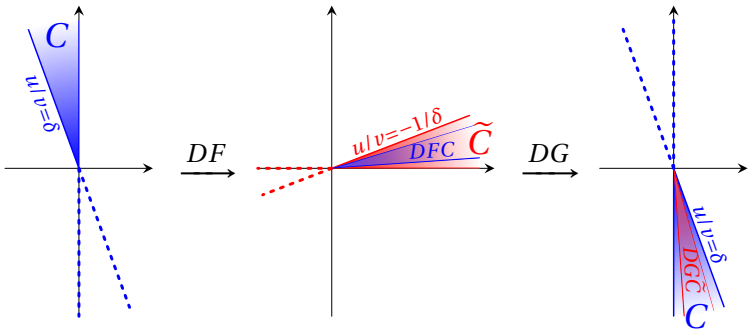

FIGURE 7. Cones

As in Figure 7, we establish hyperbolicity of $T\restriction\Lambda$ by showing that the cone family

$$C(z):=\left\{(u,v)\in T_z\Lambda\,\middle|\,0\ge\frac{u}{v}\ge\underbrace{\delta:=-\frac{\Delta}{2}+\sqrt{\left(\frac{\Delta}{2}\right)^2-1}}_{\text{so }\delta^2+\Delta\delta+1=0,\text{ that is, }\boxed{\delta+\Delta=-1/\delta}}>-1\right\}$$

for $z\in\Lambda$ is strictly DT-invariant. To that end, note first that

$$DFC\subsetneq\widetilde{C}(z):=\left\{(u,v)\in T_z\Lambda\,\middle|\,u/v\ge-1/\delta=\delta+\Delta\right\}$$

because if $(u,v)\in C(x,y)$, then

$$(u',v'):=DF_{(x,y)}(u,v)=(u+\mathfrak{f}'(y)v,v),\quad\text{so}\quad\frac{u'}{v'}=\frac{u}{v}+\mathfrak{f}'(y)>\frac{u}{v}+\Delta\ge\delta+\Delta.$$

Next, note that $DG\widetilde{C}\subsetneq C$ since $(u,v)\in\widetilde{C}(x,y)\Rightarrow(u',v'):=DG(u,v)=(u,v-\mathfrak{f}'(y)u)$, so

$$\frac{u'}{v'}=\frac{u}{v-\mathfrak{f}'(y)u}=\frac{1}{\underbrace{\underbrace{\frac{v}{u}}_{\le-\delta<1}-\underbrace{\mathfrak{f}'(y)}_{>\Delta>2}}_{<0}}>\frac{1}{-\delta-\Delta}=\delta.$$

Thus, $DTC=\pm DGDFC\subset C$ strictly, as claimed . Together with area-preservation ([5, Theorem 5.1.15], or by a simple calculation), this also implies that DT uniformly expands vectors in C, which verifies the cone criterion for uniform hyperbolicity.

Note from the computations or from Figure 7 that DT flips the cones "half the time". This feature of the counter-orientation of the self-linked twist and Figure 7 illustrate that hyperbolicity requires the twists to be strong enough.

Remark 1. Figure 7 and a look at linear parts illustrate the relative delicacy in handling counter-oriented twists. In this situation, the linear parts can be taken to be

$$DF = \begin{pmatrix} 1 & a \\ 0 & 1 \end{pmatrix}, \qquad DG = \begin{pmatrix} 1 & 0 \\ -a & 1 \end{pmatrix}, \qquad DG\,DF = \begin{pmatrix} 1 & 0 \\ -a & 1 \end{pmatrix}\begin{pmatrix} 1 & a \\ 0 & 1 \end{pmatrix} = \begin{pmatrix} 1 & a \\ -a & 1-a^2 \end{pmatrix}.$$

The latter has eigenvalues $\lambda_\pm = 1 - \frac{a^2}{2} \pm \frac{a}{2}\sqrt{a^2-4} < 1$; these lie on either side of -1 *when* $a > 2$, but hyperbolicity can fail for smaller a. It is well to add that this does not require $\mathfrak{f}'$ to be constant; if $ab > 4$ then

$$\begin{pmatrix} 1 & 0 \\ -b & 1 \end{pmatrix}\begin{pmatrix} 1 & a \\ 0 & 1 \end{pmatrix} = \begin{pmatrix} 1 & a \\ -b & 1-ab \end{pmatrix}$$

has eigenvalues $\lambda_\pm = 1 - \frac{ab}{2}\left(1 \pm \sqrt{1-\frac{4}{ab}}\right)$ on either side of -1:

$$\lambda_+ = 1 - \underbrace{\frac{ab}{2}}_{>2}\left(\underbrace{1+\sqrt{1-\frac{4}{ab}}}_{>1}\right) < -1 \quad \text{and} \quad \lambda_- = \frac{1}{\lambda_+} > -1.$$

By contrast, for co-oriented twists this becomes

$$\begin{pmatrix} 1 & 0 \\ b & 1 \end{pmatrix}\begin{pmatrix} 1 & a \\ 0 & 1 \end{pmatrix} = \begin{pmatrix} 1 & a \\ b & 1+ab \end{pmatrix}$$

with eigenvalues $\lambda_\pm = 1 + \frac{ab}{2}\left(1 \pm \sqrt{1+\frac{4}{ab}}\right) > 0$ on either side of 1 *whenever* $ab > 0$. Indeed, a picture corresponding to Figure 7 for this situation shows strict invariance of the first quadrant for any $a, b > 0$ (both twists preserve the first quadrant, and its image under the composition is the cone bounded by the columns of this last matrix, which are positive).

6. Further work

6.1. Contact homology. Returning to the fact that this construction can be carried out entirely in the realm of contact flows, we first point to amplifications analogous to the aims in [7]: it would be interesting[2] to associate with these surgered flows some insights into exponential orbit growth produced by cylindrical contact homology for any Reeb flow with the same contact structure.

6.2. Transitivity, and ergodicity of Liouville measure. Geometrically, a natural direction for extensions is to develop ways in which a flow built in this way is (nonuniformly) hyperbolic on the entire manifold rather than retaining periodic pieces. It seems plausible that choosing several surgery annuli built from self-intersecting geodesics in such a way that their footpoint projections cover the surface, would "in general" produce hyperbolicity of Liouville measure if the corresponding surgeries are carried out at the same time. However, handling the interactions between the annuli is likely to be technically daunting.

A lesser issue is the choice of geodesic in Figure 1. It is clear that this is inessential for the arguments in Sections 3 that produce the invariant set. It is a more significant convenience in Sections 4 and 5. At the level of precision needed here, an adaptation of the coordinate choices produces like local computations and the desired conclusion. However, for producing contact flows, one needs to choose Darboux coordinates on the embedded surgery annulus in order to directly implement the surgery description in [6, 7]. For establishing hyperbolicity of a horseshoe in Section 5, this is an inessential convenience, but for establishing hyperbolicity of Liouville measure (restricted to the

[2] But daunting, as noted there: "The growth rate of contact homology appears quite difficult to handle" in the present case [7, Remark 3.15].

surgered part of the flow), this seems more urgent. It may be worth noting that the arguments in Section 5 will work when the twists are not at right angles, possibly requiring stronger twisting. Here it is relevant that the twisting by the differential of the surgery identification is inversely proportional to the width of the surgery annulus, averting the need for changing the degree of the Dehn twist. (At the same time, "thinner" twists may have to be more numerous to cover the manifold.)

References

[1] Robert Burton and Robert W. Easton. Ergodicity of linked twist maps. In *Global theory of dynamical systems (Proc. Internat. Conf., Northwestern Univ., Evanston, Ill., 1979)*, volume 819 of *Lecture Notes in Math.*, pages 35–49. Springer, Berlin, 1980.

[2] Vincent Colin, Pierre Dehornoy, and Ana Rechtman. On the existence of supporting broken book decompositions for contact forms in dimension 3, 2020.

[3] Robert L. Devaney. Subshifts of finite type in linked twist mappings. *Proc. Amer. Math. Soc.*, 71(2):334–338, 1978.

[4] Robert L. Devaney. Linked twist mappings are almost Anosov. In *Global theory of dynamical systems (Proc. Internat. Conf., Northwestern Univ., Evanston, Ill., 1979)*, volume 819 of *Lecture Notes in Math.*, pages 121–145. Springer, Berlin, 1980.

[5] Todd Fisher and Boris Hasselblatt. *Hyperbolic flows*. Zurich Lectures in Advanced Mathematics. European Mathematical Society (EMS), Zürich, 2019.

[6] Patrick Foulon and Boris Hasselblatt. Contact Anosov flows on hyperbolic 3-manifolds. *Geom. Topol.*, 17(2):1225–1252, 2013.

[7] Patrick Foulon, Boris Hasselblatt, and Anne Vaugon. Orbit growth of contact structures after surgery. *Ann. H. Lebesgue*, 4:1103–1141, 2021.

[8] Matthew Nicol. A Bernoulli toral linked twist map without positive Lyapunov exponents. *Proc. Amer. Math. Soc.*, 124(4):1253–1263, 1996.

[9] Matthew Nicol. Stochastic stability of Bernoulli toral linked twist maps of finite and infinite entropy. *Ergodic Theory Dynam. Systems*, 16(3):493–518, 1996.

[10] Feliks Przytycki. Ergodicity of toral linked twist mappings. *Ann. Sci. École Norm. Sup. (4)*, 16(3):345–354 (1984), 1983.

[11] J. Springham and R. Sturman. Polynomial decay of correlations in linked-twist maps. *Ergodic Theory Dynam. Systems*, 34(5):1724–1746, 2014.

[12] James Springham. Ergodic properties of linked-twist maps, 2008.

[13] James Springham and Stephen Wiggins. Bernoulli linked-twist maps in the plane. *Dyn. Syst.*, 25(4):483–499, 2010.

[14] Rob Sturman, Julio M. Ottino, and Stephen Wiggins. *The mathematical foundations of mixing*, volume 22 of *Cambridge Monographs on Applied and Computational Mathematics*. Cambridge University Press, Cambridge, 2006. The linked twist map as a paradigm in applications: micro to macro, fluids to solids.

[15] Maciej Wojtkowski. Linked twist mappings have the K-property. In *Nonlinear dynamics (Internat. Conf., New York, 1979)*, volume 357 of *Ann. New York Acad. Sci.*, pages 65–76. New York Acad. Sci., New York, 1980.

Boris Hasselblatt: Department of Mathematics, Tufts University, Medford, MA 02155, USA
E-mail: Boris.Hasselblatt@tufts.edu

Curtis Heberle: Department of Mathematics, Tufts University, Medford, MA 02155, USA
E-mail: Curtis.Heberle@tufts.edu